THE ASTROPHYSICAL JOURNAL, 313:662–673, 1987 February 15

SIMULTANEOUS MULTIFREQUENCY OBSERVATIONS OF THE BL LACERTAE OBJECT MARKARIAN 421

F. MAKINO,[1] Y. TANAKA,[1] M. MATSUOKA,[1] K. KOYAMA,[1] H. INOUE,[1] K. MAKISHIMA,[1] R. HOSHI,[2] S. HAYAKAWA,[3] Y. KONDO,[4] C. M. URRY,[5] S. L. MUFSON,[6] K. R. HACKNEY,[7] R. L. HACKNEY,[7] S. KIKUCHI,[8] Y. MIKAMI,[8] W. Z. WIŚNIEWSKI,[9] N. HIROMOTO,[10] M. NISHIDA,[11] J. BURNELL,[12] P. BRAND,[12] P. M. WILLIAMS,[13] M. G. SMITH,[13] F. TAKAHARA,[14] M. INOUE,[14] M. TSUBOI,[15] H. TABARA,[16] T. KATO,[16] M. F. ALLER,[17] AND H. D. ALLER[17]

Received 1986 February 24; accepted 1986 August 8

ABSTRACT

Simultaneous multifrequency observations of the BL Lac object Mrk 421 covering radio through X-ray wavelengths were performed on two occasions separated by 5 weeks in 1984 January and March, and each observation was coordinated for about 1 week. We obtained composite multifrequency spectra of the central nonthermal component at the two epochs after subtracting the optical and infrared light of the underlying galaxy. The spectra show the gradual steepening toward high frequency; the power law indices are ~ 0.1, ~ 0.6, and ~ 1.0 for radio, infrared-optical, and UV bands, respectively. The UV and optical-infrared fluxes decreased by $\sim 20\%$ in 5 weeks, while the radio flux remained stable. The X-ray flux decreased by a factor of ~ 2, and the change was more pronounced at hard X-rays, which suggest that X-ray emission possibly consists of two components. The degree of polarization at the optical band varied on the time scale of a few days, while the position angle remained unchanged.

Physical parameters of Mrk 421 are discussed in terms of the synchrotron self-Compton model. Taking the spectral turnover between infrared and radio for synchrotron self-absorption, the radio emission originates in a more extended region than the infrared to X-ray emission, the source size of which should be less than $\sim 10^{-2}$ milliarcseconds. Relativistic beaming is required if the angular size is smaller than a few times 10^{-3} milliarcseconds. A possible explanation of the spectral change during the two epochs is also discussed.

Subject headings: BL Lacertae objects — galaxies: individual — galaxies: X-rays — polarization — radiation mechanisms — radio sources: galaxies

I. INTRODUCTION

The central problem of active galactic nuclei (AGNs) is the emission mechanism of the continuum radiation at radio through gamma-ray frequencies, and the ultimate energy source of that radiation. Apparently these AGNs somehow generate very high luminosities (assuming cosmological distances and isotropic emission) inside very small volumes (as deduced from variability time scales). BL Lac objects are distinguished from other classes of AGNs by their rapid variability, high degree of polarization, and general lack of discrete spectral features. These properties are useful diagnostics of the radiation processes. Simplified models such as the synchrotron self-Compton model with or without relativistic beaming have been proposed to explain many of the observed characteristics of BL Lac objects and other AGNs. A high degree of polarization in the infrared and optical region may be evidence of a synchrotron process, a hypothesis that can be strengthened if correlated temporal changes in radio, infrared, and optical bands are detected. Many AGNs have been observed simultaneously in various frequency bands from radio to X-ray frequencies in order to search for correlated variations within an individual spectrum (Kondo *et al.* 1981; Bregman *et al.* 1982, 1984; Worrall *et al.* 1982, 1984*a*, *b*, *c*; Wills *et al.* 1983; Mufson *et al.* 1984; Glassgold *et al.* 1983; Hutter and Mufson 1986). The absence of discrete spectral features, often a nuisance when determining the physical state of the emitting region, in this case provides a conveniently uncontaminated broad-band spectrum.

Mrk 421 was first noted as a blue excess object which turned out to be an elliptical galaxy with a bright, pointlike nucleus. The redshift of the galaxy was measured to be $z = 0.03$ (Ulrich *et al.* 1975), but the spectrum of the nucleus was featureless. It also showed the optical polarization and flat radio spectrum, common to BL Lac objects (Maza, Martin, and Angel 1978; O'Dell *et al.* 1978*a*). The angular size of the radio source associated with Mrk 421 is less than 1 milliarcsecond (mas) at 6 cm (Weiler and Johnston 1980; Baath *et al.* 1981). The ultraviolet emission from Mrk 421 has been monitored over the past 7 yr with the *International Ultraviolet Explorer* (*IUE*) satellite. Nine *IUE* spectra obtained between 1978 and 1981 showed some variability, but no or only very weak correlation between flux level and spectral index (Ulrich *et al.* 1984). Since it is one of the brightest BL Lac objects known in the X-ray

[1] Institute of Space and Astronautical Science, Tokyo.
[2] Department of Physics, Rikkyo University.
[3] Department of Astrophysics, Nagoya University.
[4] NASA/Goddard Space Flight Center.
[5] Center for Space Research, Massachusetts Institute of Technology.
[6] Astronomy Department, Indiana University.
[7] Department of Physics and Astronomy, Western Kentucky University.
[8] Tokyo Astronomical Observatory, University of Tokyo.
[9] Lunar and Planetary Laboratory, University of Arizona.
[10] Radio Research Laboratory, Tokyo.
[11] Department of Physics, Kyoto University.
[12] Astronomy Department, University of Edinburgh.
[13] Royal Observatory Edinburgh.
[14] Nobeyama Radio Observatory, University of Tokyo. The Nobeyama Radio Observatory, a branch of the Tokyo Astronomical Observatory, University of Tokyo, is a cosmic radio observing facility open for outside users.
[15] Department of Astronomy, University of Tokyo.
[16] Faculty of Education, Utsunomiya University.
[17] Radio Astronomy Observatory, University of Michigan.

band, Mrk 421 has been observed fairly often with various X-ray instruments (see summary of observations and references in Urry, Mushotzky, and Holt 1986). X-ray observation of Mrk 421 with the *HEAO 1* satellite detected a change in spectral index from 2.1 to 3.9 and the disappearance of the hard component above 10 keV by comparing with earlier observations from the *OSO 8* and *SAS 3* satellites (Mushotzky *et al.* 1979). Because of the lack of simultaneity among the observations at radio through X-ray frequencies, correlations among intensity changes have been poorly studied.

We made simultaneous multifrequency observations of the BL Lac object Mrk 421 at radio, infrared, optical, ultraviolet, and X-ray frequencies on two occasions in 1984 January and March. In § II we summarize observations performed at each frequency band, and we describe the composite spectrum thus obtained at each of the two epochs. In § III interrelations among various observed bands and the comparisons with previous observations are discussed. In § IV an interpretation of those results in terms of the synchrotron self-Compton model is attempted. Conclusions will follow in § V.

II. OBSERVATIONS

The observation was conducted at the radio, infrared, optical, ultraviolet, and X-ray bands on two occasions separated by 5 weeks, 1984 January and March. The coverage of the observed frequency bands and the instruments utilized in the present observations are summarized in Table 1.

a) X-Ray Observations

X-rays were observed with two sets of the scintillation proportional counters (SPC-A and SPC-B) on board the *Tenma* satellite (Tanaka *et al.* 1984; Koyama *et al.* 1984). The observed energy range was 1.5–35 keV, but above $\sim$10 keV, the flux was too faint to discriminate from the background. The day-to-day variations of the integrated energy flux over the energy range 1.5–10 keV are depicted in the lowest panel of Figure 1. The statistical accuracy of day-to-day data was not good enough to obtain the energy spectrum. Then we summed up the data for each observation period; the time-averaged energy spectra observed in January and March are shown in Figure 2.

The flux decreased by a factor of $\sim$2 from January to March. Particular attention has been paid to the spectral analysis, since for faint sources such as Mrk 421 the spectral shapes depend critically on background subtraction. The properties of the background spectrum have long been studied carefully using extensive data sets compiled from *Tenma* (Koyama *et al.* 1984). Before summing the data from SPC-A and SPC-B, the spectral analysis was independently carried out for each datum to check the consistency of the results. The spectra obtained independently from SPC-A and SPC-B were combined to improve statistics, after confirmation of consistency. The best-fit power-law index for the January and March observations over 1.5–10 keV is 1.1 ± 0.2 and 1.8 ± 0.3, with the normalization factor $(1.01 \pm 0.17) \times 10^{-2}$ keV cm^{-2} s^{-1} keV^{-1} and $(8.7 \pm 2.4) \times 10^{-3}$ keV cm^{-2} s^{-1} keV^{-1} at 1 keV, respectively.

It is, however, to be noticed that the single power-law fit is only marginally acceptable, since the reduced χ^2 value is 2.3 (degree of freedom, 11) and 2.2 (degree of freedom, 7) for the January and March data, respectively. The deviations from the single power-law models are evident above 4 keV. The spectrum obtained in January is flatter above 4 keV as compared to March observations. Below 4 keV, on the other hand, the spectral index is 1.6 ± 0.1 and 1.7 ± 0.2, respectively, while the intensity varied by a factor of 2.

We notice that the *EXOSAT* satellite also observed Mrk 421 in the period 1984 February 1–6, 1 week after our January observation (Warwick, McHardy, and Pounds 1985). The intensity and spectral index are intermediate between those of our January and March observations.

b) UV Observations

Ultraviolet observations were made by the short-wavelength prime (SWP) and the long-wavelength prime (LWP) cameras of the *IUE* satellite on five occasions during the present program. The results are summarized in Table 2. The integrated fluxes are plotted in the fifth panel of Figure 1. The

TABLE 1

ORGANIZATION OF OBSERVATIONS

Observatory	Band	Observers
Tenma	X-ray 1.5–30 keV	F.M., Y.T., M.M., K.K., H.I., K.M., R.H., S.H.
IUE	UV 1200–3000 Å	Y.K., C.M.U., S.L.M., K.R.H., R.L.H.
Mt. Lemon	Optical *U, B, V, R, I*	W.Z.W.
Okayama ..... Dodaira	Optical *U, B, V, R* with polarimetry	S.K., Y.M.
Agematsu	IR *J, H, K*	N.H., M.N.
UKIRT	IR *J, H, K, L, L', M, N* with *J, H, K* polarimetry	J.B., P.B., P.M.W., M.G.S.
NRO	Radio 10, 22, 43 GHz	F.T., M.I., M.T., H.T., T.K
Michigan	Radio 4.8, 8.0, 14.5 GHz	M.F.A., H.D.A.

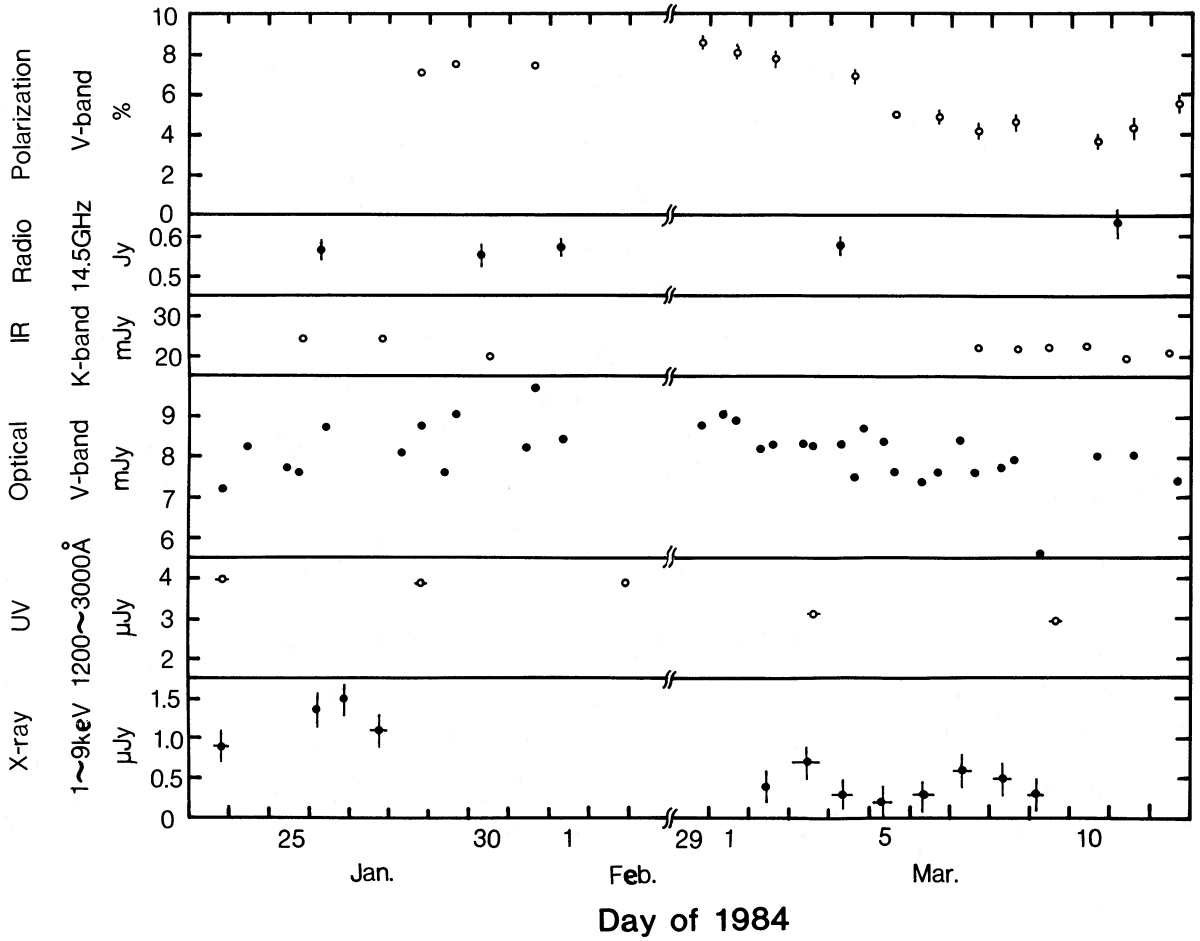

FIG. 1.—Light curves of the nonthermal component of Mrk 421. First panel shows that of the degree of polarization at the V band. Following panels show that of fluxes in the radio (14.5 GHz), IR (K band), optical (V band), UV and X-ray frequencies, respectively.

TABLE 2

RESULTS OF UV OBSERVATIONS BY *IUE*

Data (1984)	Image	A^a (mJy)	α^b	χ^2/DOF	Integrated Flux[c]
Jan 23.....	LWP 2669 LWP 2700 SWP 22082	6.65 ± 0.12	1.04 ± 0.04	0.71	6.01 ± 0.11
Jan 28.....	LWP 2711 LWP 2712 SWP 22128	6.35 ± 0.20	1.01 ± 0.07	0.55	5.82 ± 0.11
Feb 2	LWP 2732	6.77 ± 0.15	1.13 ± 0.20	0.11	5.88 ± 0.18
Mar 3	LWP 2881 LWP 2882 SWP 22398	5.24 ± 0.18	1.10 ± 0.08	1.09	4.61 ± 0.16
Mar 9	LWP 2915 SWP 22445	5.04 ± 0.21	1.12 ± 0.08	0.47	4.38 ± 0.14

[a] Flux density at 3000 Å.
[b] Spectral index for 1200–3000 Å.
[c] Integrated over 1200–3000 Å and in units of 10^{-11} ergs cm^{-2} s^{-1}.

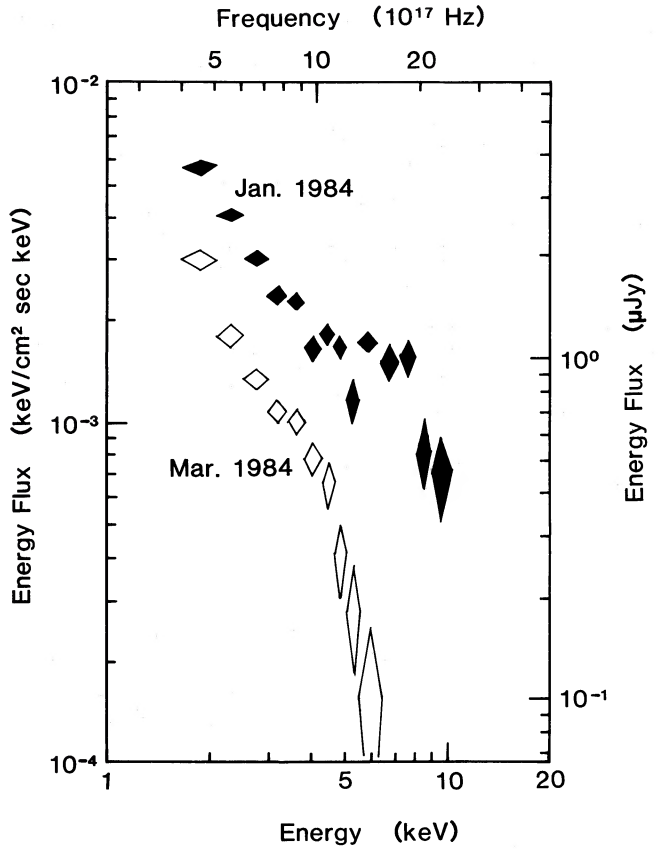

FIG. 2.—X-ray spectra obtained by *Tenma*. Data were integrated over each observation period.

spectra were extracted from the line-by-line file using a customized narrow slit to maximize the signal to noise. Data points contaminated by reseaux or cosmic-ray hits were removed, and the data were then binned in intervals of ~25 Å. The binned data points were weighted according to the rms deviations within the bins and were fitted to a power-law spectrum using a least-squares procedure for 1200–3000 Å range.

It is to be noted that the integrated ultraviolet flux decreased by 20%–30% from January to March, and the spectral index α shows a slight steepening (a change of α of ~0.1).

c) *Optical Observations*

Optical observations were made at the Okayama Astrophysical Observatory, the Dodaira Station, and the Mount Lemon Observatory. Five telescopes were used with various diaphragm sizes, which are listed in Table 3.

Mrk 421 is found at the core of a giant elliptical galaxy, and, in particular, optical and infrared fluxes are contaminated by galaxy emission. Therefore, we must subtract the galaxy component to obtain the flux from the central compact core. The distribution of the surface brightness of the galaxy was studied by Kinman (1978), Mufson *et al.* (1980), and Hickson *et al.* (1982), but some discrepancies remained among their results. Kikuchi and Mikami (1986) also made the multiaperture photometry of Mrk 421 and obtained a result similar to that by Kinman (1978). In the present study, the subtraction of the contribution from the underlying galaxy has been made using the results by Kikuchi and Mikami (1986). The corrections for the apertures used in the observations are also tabulated in Table 3. The colors of the underlying galaxy are taken to be constant as $U-B = 0.46$, $B-V = 1.05$, and $V-R = 0.90$ after Kikuchi and Mikami (1985). These colors are consistent with those of a redshifted elliptical galaxy at $z = 0.03$. For $R-I$, the mean value of 0.78 for elliptical galaxies (Johnson 1966) is assumed, since the measurement of the underlying galaxy has yet to be made at the I band.

The observed fluxes and the fluxes of the nonthermal component are tabulated in Table 4. The day-to-day variation of the flux of the nonthermal component at the V band is shown in the fourth panel of Figure 1. The nominal errors associated with the observed fluxes are typically 2%–3% but 1% for several cases at Dodaira in March. However, the derived flux of the nonthermal component shows a scatter greater than the observational errors, reaching ~10%, depending on the aperture and/or telescope. A part of this scatter is certainly caused by the incompleteness of the subtraction of the galaxy contribution. Although we have no reasonable explanation for the remaining scatter, we suspect that the seeing condition and the scattered light of a nearby 6 mag star affect the measurement of the extended source and of the sky brightness, respectively.

Continuum spectra for both observing periods, as well as those in the infrared region, are shown in Figure 3. In the January data of the fluxes in the B and V bands, we find a systematic difference between the data obtained by the 100 cm telescope at Mount Lemon and those by the 188 cm telescope at Okayama, although the spectral indices coincided well with each other. The difference amounts to 7%, and the origin of the difference is unknown. For the spectra in the March epoch, we used the results after March 4, since the optical flux abruptly decreased around March 3 but was stable thereafter.

The average V band intensities in January and March were 8.9 ± 0.5 mJy and 7.8 ± 0.5 mJy, respectively. The spectral

TABLE 3

LIST OF TELESCOPES FOR OPTICAL OBSERVATIONS AND APERTURE CORRECTION FOR THE UNDERLYING GALAXY

Observatory	Diameter (cm)	Aperture	Date (1984)	Aperture Correction V Magnitude
Okayama	91	37.″1	Jan 23	13.82
		27.9	Jan 29, Mar 3, 4, 6	14.05
	188	8.9	Jan 29, 31	14.98
		11.8	Jan 28	14.72
Dodaira	91	18	Feb 7, 29	14.39
		13	Feb 6, 9, Mar 1–12	14.65
Mt. Lemon	100	29.7	Jan 24–Feb 1, Mar 9	14.00
	150	12.4	Mar 1–8	14.68

TABLE 4

OBSERVED OPTICAL FLUXES AND DERIVED FLUXES OF NONTHERMAL COMPONENT

DATE 1984 (UT)	APERTURE	OBSERVED F(U)	F(B)	F(V) (mJy)	F(R)	F(I)	NONTHERMAL F(U)	F(B)	F(V) (mJy)	F(R)	F(I)
Okayama											
Jan 23.80	37".1	8.96	12.25	18.69	...	...	7.61	7.51	7.22	...	...
25.74	27.9	8.40	11.70	16.89	...	...	7.31	7.86	7.61	...	...
28.80	11.8	7.94	9.91	13.79	19.52	...	7.36	7.84	8.79	10.60	...
29.64	8.9	7.73	9.56	13.05	17.81	...	7.27	7.93	9.11	10.78	...
31.65	8.9	8.40	10.38	13.67	17.48	...	7.93	8.75	9.73	10.46	...
Mar 3.53	27.9	7.38	11.07	17.53	...	...	6.29	7.23	8.24	...	...
4.82	27.9	7.05	10.58	18.02	...	...	5.96	6.74	8.73	...	...
6.74	27.9	7.31	10.29	16.89	...	...	6.23	6.45	7.61	...	...
Mt. Lemon											
Jan 24.43	29.7	...	11.38	18.02	...	...	.....	7.36	8.30	...	...
25.40	29.7	...	11.07	17.53	...	...	...	7.05	7.81	...	...
26.43	29.7	...	11.70	18.52	...	...	...	7.68	8.80	...	...
28.33	29.7	...	10.77	17.85	...	...	...	6.75	8.13	...	...
29.39	29.7	...	11.38	17.37	...	...	...	7.36	7.65	...	...
31.44	29.7	...	11.38	18.02	...	...	...	7.36	8.30	...	...
Feb 1.34	29.7	...	11.70	18.18	...	...	...	7.68	8.46	...	...
Mar 1.35	12.4	7.25	9.73	14.31	20.44	27.64	6.64	7.58	9.12	11.18	12.31
2.26	12.4	6.79	9.38	13.42	20.26	27.39	6.18	7.23	8.22	11.00	12.06
3.34	12.4	6.67	9.04	13.54	19.52	27.14	6.06	6.89	8.35	10.26	11.81
4.31	12.4	6.67	8.88	13.54	19.34	26.64	6.06	6.73	8.35	10.09	11.31
5.36	12.4	...	9.04	14.05	...	...	...	6.89	8.85	...	...
6.30	12.4	6.25	8.64	12.58	18.82	25.45	5.64	6.49	7.38	9.56	10.11
7.26	12.4	6.73	8.88	13.67	19.70	25.68	6.12	6.73	8.47	10.45	10.35
8.30	12.4	6.25	8.56	12.93	18.65	25.92	5.64	6.41	7.74	9.39	10.59
9.29	29.7	...	9.38	15.27	...	...	...	5.36	5.54	...	...
Dodaira											
Feb 6.79	13.0	8.27	10.67	15.23	22.08	...	7.65	8.46	9.89	12.56	...
7.83	18.0	9.42	11.95	17.55	25.25	...	8.63	9.14	10.76	13.15	...
9.78	13.0	8.58	10.86	15.91	22.66	...	7.96	8.65	10.56	13.14	...
29.76	18.0	7.72	10.29	15.56	22.43	...	6.92	7.48	8.77	10.34	...
Mar 1.65	13.0	7.29	9.68	14.22	20.46	...	6.66	7.47	8.87	10.94	...
2.60	13.0	7.03	9.26	13.62	19.61	...	6.40	7.05	8.28	10.09	...
4.63	13.0	6.25	8.40	12.82	18.80	...	5.62	6.19	7.48	9.28	...
5.64	13.0	6.36	8.55	12.93	18.80	...	5.74	6.34	7.59	9.28	...
6.71	13.0	6.30	8.55	12.93	18.80	...	5.68	6.34	7.59	9.28	...
7.68	13.0	6.36	8.55	12.93	18.64	...	5.74	6.34	7.59	9.13	...
8.61	13.0	6.66	8.86	13.27	19.12	...	6.03	6.65	7.93	9.60	...
10.68	13.0	6.54	8.78	13.39	19.44	...	5.91	6.57	8.04	9.93	...
11.60	13.0	6.78	9.02	13.39	19.28	...	6.15	6.81	8.04	9.76	...
12.71	13.0	6.48	8.70	12.82	18.64	...	5.85	6.49	7.48	9.13	...

index in the *UVBR* region varied from 0.65 ± 0.15 to 0.76 ± 0.10 from January to March. Slight darkening and spectral steepening are barely significant, if we consider only the data in the optical region. It should be also noted that, in early February, a brightening to 10.4 ± 0.3 mJy in the *V* band with a spectral index of 0.72 ± 0.06 has been observed at Dodaira.

Optical polarimetry was also made simultaneously with the photometry by the 188 cm telescope at Okayama, and by the 91 cm telescope at Dodaira. The polarization of the nonthermal component showed no wavelength dependence in the *UBVR* region throughout the whole observing period, provided that the light from the underlying galaxy was unpolarized. The polarization properties of the nonthermal component through the *U* to *K* bands averaged over March 8–12 are given in Table 5. No wavelength dependence of the degree of polarization was found in the optical and near-infrared regions.

The variation of the degree of the polarization is shown in the first panel of Figure 1. The degree of polarization showed a considerable change during the March epoch; from February 29 to March 5 the degree of polarization was as high as 7%–8.5%, with a trend of the smooth weakening, and on March 6 it declined abruptly to 4%–5%, while the position angle remained constant at 170°–180°. This abrupt change of the polarization seems to be correlated with the flux decrease in the same period.

d) Infrared Observations

Infrared observations were made with the 3.8 m telescope at United Kingdom Infrared Telescope (UKIRT) at Mauna Kea, Hawaii, and the 1 m telescope at the Agematsu Infrared Observatory. At Agematsu we observed Mrk 421 on January 25 and 27 and March 7 and 8 with a rectangular aperture of 24″ in the

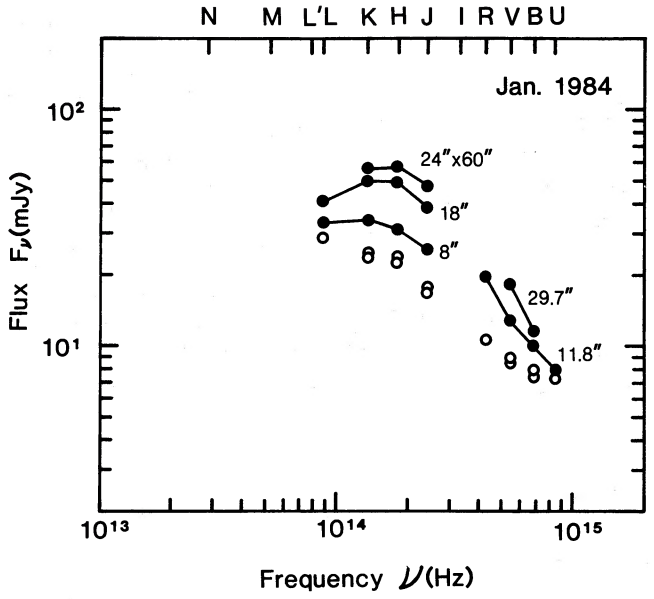

FIG. 3a

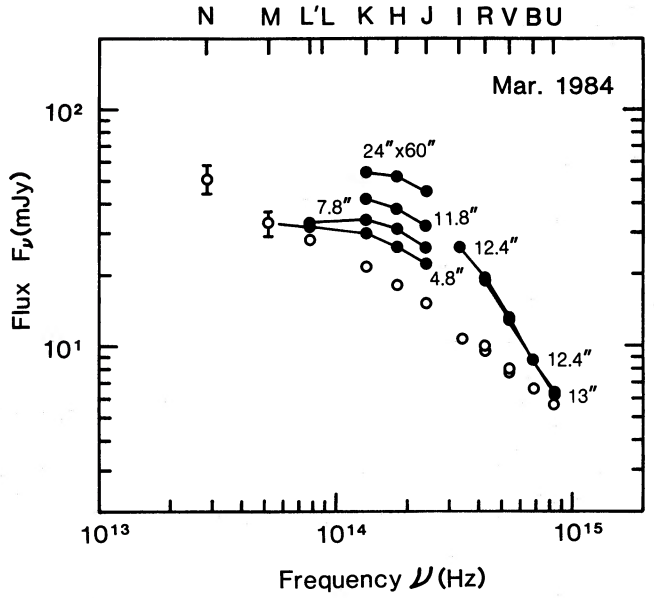

FIG. 3b

FIG. 3.—IR-optical spectra of Mrk 421 in 1984 January–February (*a*) and in March (*b*). *Filled circles with straight lines*: observed fluxes. Beam sizes are also shown numerically in the figure. *Open circles*: derived nonthermal fluxes.

right ascension by 60″ in the declination and 40″ chopping throw at the *J*, *H*, and *K* bands. The calibration was made by using ξ UMa as a standard star and SAO 062387 as a reference star. UKIRT observations were made on February 4 and 6 at the *J*, *H*, *K*, and *L* bands with a 18″ aperture using GL 299 as a reference star. On March 8–12, the *J*, *H*, *K*, and *L'* band observations were made with 4.″8, 7.″8, and 11.″8 apertures, on March 11–12 the *M* band observation was made with a 4.″8 aperture, and on March 8–10 the *N* band observation was made with a 6″ aperture. On January 30, photometry at *J*, *H*, *K*, and *L* bands was made with a 8″ aperture using the NASA infrared telescope, at Mauna Kea, Hawaii.

The observed data are tabulated in Table 6. The infrared flux decreased by 13% ± 4% from January to March, comparing the Agematsu observations at two epochs. As in the optical observations, the contribution of the underlying galaxy was subtracted to obtain the fluxes of the central nonthermal component for *J*, *H*, *K*, *L* (*L'*) bands. Since the observation with the largest beam size of 24″ × 60″ does not agree with the brightness of the model galaxy, we obtain contrariwise the brightness of the underlying galaxy for the 24″ × 60″ beam size by subtracting the nonthermal component derived from the observations with smaller beam sizes on March 8, and apply it to the photometry in the January epoch. The infrared colors of the underlying galaxy are obtained as $J-H=0.69$ and $H-K=0.40$ from the observations in March, which become almost consistent with those of typical elliptical galaxies (Frogel *et al.* 1975; Persson, Frogel, and Aaronson 1979; Glass 1984), taking account of the *K*-corrections (Frogel *et al.* 1978). We assumed $K-L=0.06$ (Aaronson 1978) and $V-K=3.40$ (Aaronson 1978; Persson, Frogel, and Aaronson 1979), consistent with those of typical elliptical galaxies including *K*-corrections. For the *M* and *N* bands the contribution of the galaxy is safely neglected. The resulting fluxes of the nonthermal component are summarized in the bottom panel of Table 6, and the flux at the *K* band is plotted in the third panel of Figure 1. The spectra obtained for respective epochs are shown in Figure 3, along with the optical spectra. The spectral index in the infrared band was 0.5 ± 0.2 and 0.57 ± 0.11 for January and March, respectively. The conversion of the magnitude to the absolute flux has been made using coefficients tabulated in Table 6, on the basis of the calibration by Blackwell *et al.* (1983).

The polarization measurements were also made on March 9, 11, and 12 at the *J*, *H*, and *K* bands by UKIRT. Those results are tabulated in Table 5, together with the optical polarization. The degree of polarization and the position angle of the nonthermal component in the infrared are 4.8% ± 0.4% and 180° ± 5°, which are fully consistent with those at optical bands.

TABLE 5

POLARIZATION OF NONTHERMAL COMPONENT OBSERVED IN 1984 MARCH 8–12

Parameter	*U*	*B*	*V*	*R*	*J*	*H*	*K*
Beam size	13″	13″	13″	13″	7.″8	7.″8	7.″8
Observed degree of polarization[a]	4.0 ± 0.3	3.3 ± 0.3	3.0 ± 0.2	2.7 ± 0.2	2.5 ± 0.4	2.9 ± 0.3	2.8 ± 0.6
Degree of polarization of nonthermal component[a]	4.3 ± 0.3	4.3 ± 0.4	4.7 ± 0.4	5.0 ± 0.4	4.4 ± 0.7	5.0 ± 0.4	4.5 ± 1.0
Position angle	177° ± 2°	175° ± 3°	174° ± 2°	175° ± 3°	179° ± 9°	180° ± 5°	184° ± 13°

[a] In percent.

TABLE 6

SUMMARY OF INFRARED PHOTOMETRIC OBSERVATIONS[a]

DATE (1984) (UT)	APERTURE		*J*	*H*	*K*	*L*	*L'*	*M*	*N*
		Central frequency:	240 THz	182 THz	136 THz	86.9 THz	78.5 THz	62.7 THz	28.6 THz
		Central wavelenth:	1.25 μm	1.65 μm	2.2 μm	3.45 μm	3.82 μm	4.78 μm	10.5 μm
		Absolute flux at zero magnitude:	1540 Jy	980 Jy	670 Jy	290 Jy	250 Jy	165 Jy	40 Jy
Jan 25/27	24″ × 60″		46.94	57.44	56.24	...	...	...	...
Jan 30	8		25.56	31.28	33.89	32.69	...	...	...
Feb 4/6	18		38.7	49.1	49.4	40.4	...	...	...
Mar 7/8	24 × 60		44.83	51.91	54.21	...	...	...	...
Mar 8	4.8		22.06	26.02	30.62	...	30.90	...	...
	7.8		26.76	31.86	35.49	...	31.76	...	...
	11.8		31.88	37.95	41.50	...	...	...	...
	6		...	...	...	...	...	...	58 ± 18
Mar 9	4.8		23.52	26.74	33.27	...	35.15	...	...
	7.8		26.27	31.28	34.52	...	32.65	...	...
	6		...	...	...	...	...	...	58 ± 12
Mar 10	7.8		26.03	30.71	32.97	...	29.8	...	...
	6		...	...	...	...	...	...	36.5 ± 7
Mar 11	4.8		22.26	26.26	29.52	...	30.9	38 ± 6	...
	7.8		26.03	31.57	34.20	...	30.3	...	...
Mar 12	4.8		21.65	26.26	25.95	...	30.0	29 ± 6	...
	7.8		26.27	31.86	34.52	...	35.5	...	...
Jan 25/27	...		17.7	23.9	24.2	...	...	...	...
Feb 4/6	...		16.6	22.5	23.4	28.5	...	...	...
Mar 8/12	...		15.2	18.1	21.6	...	27.7	33.2	50.7

[a] Lowermost three rows show the fluxes of the nonthermal component in units of mJy. Errors are less than 1% unless otherwise indicated.

e) Radio Observations

Radio observations were made with the 45 m telescope at the Nobeyama Radio Observatory and the 26 m telescope at the University of Michigan. At Nobeyama, flux measurements at 10, 22, and 43 GHz were made, while at Michigan flux was measured at 4.8, 8.0, and 14.5 GHz. At Nobeyama the calibration was done by using 3C 286 as the primary calibrator of which the fluxes are 4.7, 2.6, and 1.7 Jy at 10, 22, and 43 GHz, respectively, and 3C 274, 4C 39.25, and 1144+40 were observed as references. No significant daily variations above 10% level were found, so that only the averaged data over each epoch are used. The results are listed in Table 7, from which one sees that radio fluxes are rather stable and are 570, 510, and 520 mJy at 10, 22, and 43 GHz, respectively, throughout the January and March observations.

TABLE 7

A. NRO 45 METER RADIO OBSERVATIONS[a]

Epoch (1984)	10 GHz	22 GHz	43 GHz
Jan	0.59 ± 0.03	0.47[b]	0.49 ± 0.03
Mar	0.55 ± 0.03	0.55 ± 0.05	0.55 ± 0.1

B. UNIVERSITY OF MICHIGAN 26 METER RADIO OBSERVATIONS

Epoch (1984)	4.8 GHz	8.0 GHz	14.5 GHz
Jan	0.657 ± 0.034	0.604 ± 0.013	0.540 ± 0.017
Mar	0.659 ± 0.036	0.62 ± 0.03	0.571 ± 0.020

[a] Flux density is shown in units of janskys, and errors are the standard deviation from the mean daily flux.

[b] Data are available only for 1 day, and the error cannot be estimated.

The data obtained at Michigan are consistent with those at Nobeyama, viz., 660, 610, and 550 mJy at 4.8, 8.0, and 14.5 GHz, respectively. In the second panel of Figure 1, the data at 14.5 GHz are plotted.

f) Composite Spectra

Figure 4 shows the composite energy spectra emerging from the central nonthermal component of Mrk 421 in 1984 January and March. These composite spectra are similar to those of other BL Lac objects, i.e., a power-law spectrum with a gradually increasing spectral index toward high frequencies. In the January epoch, the spectral indices are ~0.1, ~0.5, ~0.7, ~1.0, and ~1.1 for radio, IR, optical, UV, and X-ray wavelengths, respectively, while in March these are ~0.1, ~0.6, ~0.8, ~1.1, and ~1.8.

III. COMPARISON WITH PREVIOUS OBSERVATIONS

At radio wavelengths, VLBI observations (Baath *et al.* 1981; Baath 1984) revealed an unresolved core of 240 ± 40 mJy with a size less than 0.3 mas, as well as a resolved component of 270 ± 50 mJy and 3.4 mas size at 5 GHz. Other VLBI observations (Weiler and Johnston 1980; Wehrle *et al.* 1984) also revealed a compact component of ~1 mas size and ~300 mJy strength both at 5 and 2.3 GHz. There also exists a ~0.1 Jy extended component of a few arcminute size (Kapahi 1979; Ulvestad, Johnson, and Weiler 1983). Our flux measurements at radio frequencies included all these components. But the total flux of Mrk 421 was rather stable at 1 centimeter wavelength, and our value is consistent with previously reported values (Margon, Jones, and Wardle 1978; O'Dell *et al.* 1978*a*). Therefore the flux of the core component is probably ~300 mJy.

O'Dell *et al.* (1978*a*) showed that the radio spectrum extends to at least 90 GHz with a flat shape. The extrapolation of the

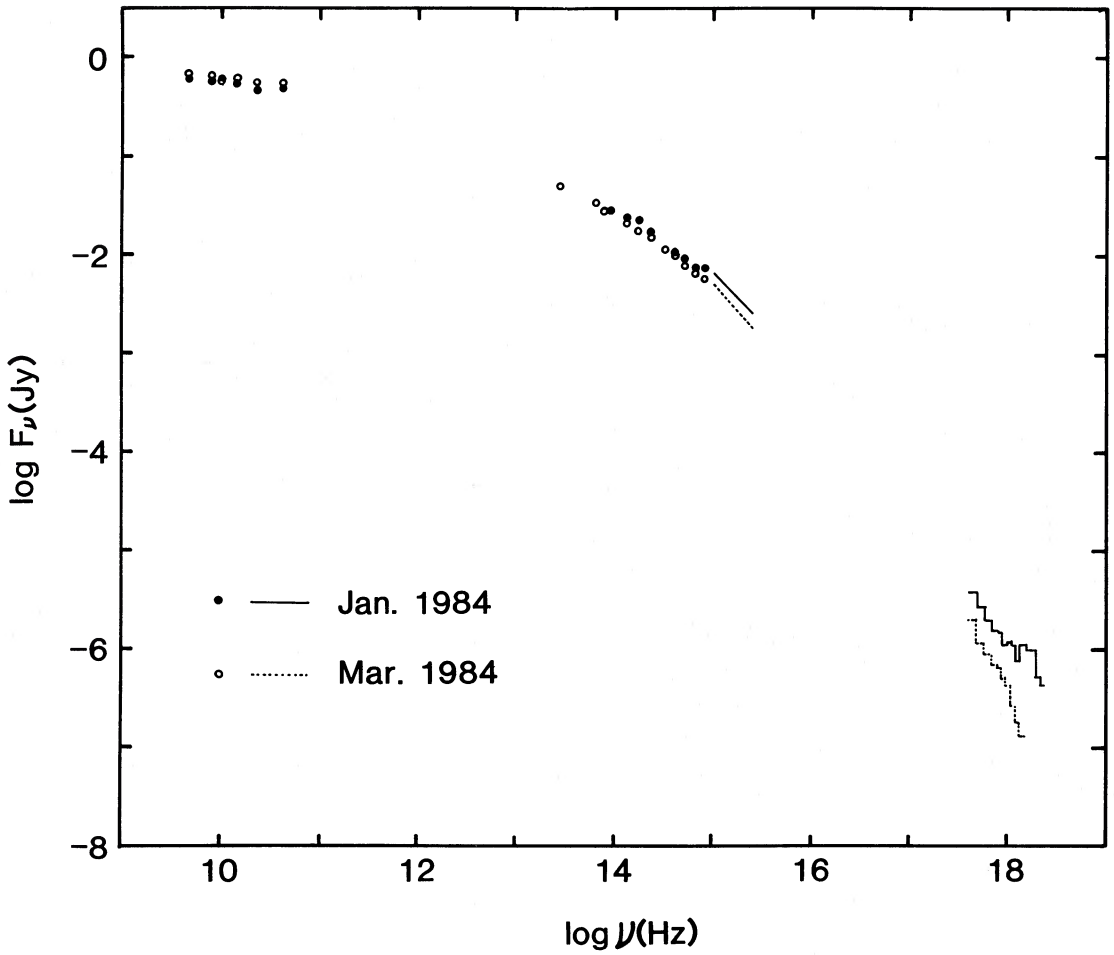

FIG. 4.—Composite spectra of the nonthermal component of Mrk 421 in 1984 January and March

flat radio spectrum of 300 mJy intersects the extrapolation of the IR-optical spectrum at $\sim 10^{12}$ Hz.

The optical fluxes were faint compared to the previous observations (Hagen-Thorn *et al.* 1983). Also the infrared fluxes of the nonthermal component were in a faint phase among previous observations at the *K* band (Ulrich *et al.* 1975; Allen 1976; Joyce and Simon 1976; O'Dell *et al.* 1978*b*; Bailey *et al.* 1981; Impey 1983). Thus we conclude that Mrk 421 was in a dark phase on two occasions of our coordinated observations.

The position angle of the optical polarization in the present observation agrees with the dominant direction in the long-term behavior (Hagen-Thorn *et al.* 1983). The polarization of Mrk 421 observed by Bailey *et al.* (1981) in 1980 December is nearly equal to that in the present observation in the position angle and the degree of polarization, although Mrk 421 was in a brighter phase then. However, Bailey *et al.* (1981) claimed that the polarization degree decreases as the wavelength increases, while our degree of polarization shows no wavelength dependence. We think it is not due to observational errors but due to the difference in the models of the underlying galaxy. Their model galaxy has the brightness by 0.3 mag smaller than that we used in the *V* band, which brings a decreasing degree of polarization as the wavelength increases through the dilution effect. Therefore, a decreasing polarization of Mrk 421 with wavelength is questionable.

It is to be noted that there exists a spectral break between IR-optical and UV bands at $\sim 10^{15}$ Hz. This spectral break or steepening seems to be common to BL Lac objects.

The UV light curve for the period 1978–1981 was analyzed by Ulrich *et al.* (1984), and they have shown that the flux varied on the time scale of a few years. In 1979 November the UV flux was in a minimum state with the spectral index of 1.0. Both the flux and the spectral index are similar to those of the present observation in 1984. Since the flux steadily increased and the spectrum hardened from 1979 to 1981, Mrk 421 might have turned to a decreasing and softening phase in 1982–1983.

The X-ray flux of this observation is significantly lower than those of previous observations by *SAS 3* (Hearn, Marshall, and Jernigen 1979) and *HEAO 1* (Mushotzky *et al.* 1979) by an order of magnitude. At those epochs X-ray fluxes were higher than or on the extrapolation from the UV spectrum. The extrapolation of the UV spectrum toward shorter wavelengths should be compared to the X-ray spectra obtained by *Tenma*. The extrapolation from the UV spectrum lies at 5.47 and 2.26 μJy at 10^{18} Hz at January and March epochs, respectively, while the observed fluxes were 1.1 and 0.51 μJy, respectively. Then the observed X-ray fluxes are lower than the extrapolation from the UV spectrum by an order of magnitude in the present observation. The spectral slope between UV and X-ray is 1.3–1.4 and is apparently steeper than the UV slope of ~ 1. On the other hand, the X-ray spectral index changes from ~ 1

at the January epoch to ~ 2 at the March epoch. Below 4 keV the X-ray spectral index was ~ 1.5 for both periods.

This result implies that X-ray emission is represented by two components. These variations of flux and spectral shape at 5 week interval are very important feature. *HEAO 1* observations in 1978 May showed a remarkable spectral change from *OSO 8* observations in 1977 May (Mushotzky *et al.* 1979). It has been suggested that the X-ray spectra of BL Lac objects have two components, a soft and a hard component (Riegler, Agrawal, and Mushotzky 1979; Worrall *et al.* 1981). We may infer that the hard component varies more violently than the soft component.

IV. IMPLICATIONS ON THE MODEL

a) Source Parameters

The continuum emission from BL Lac objects may be due to synchrotron radiation, inverse Compton scattering, or both (Blandford 1984; Konigl 1981). In this subsection we derive physical parameters of the source using the data obtained in the present observations within the context of the homogeneous and spherical symmetric synchrotron self-Compton (SSC) model (Gould 1979). The SSC model assumes the presence of relativistic electrons with power-law distribution, $N(\gamma) \propto \gamma^{-p}$ (γ is the Lorentz factor, and p is the power-law index), which emit synchrotron radiation having the power-law spectrum $S_{\rm syn} \propto \nu^{(1-p)/2}$. Since the synchrotron absorption coefficient is proportional to $\nu^{-(4+p)/2}$, the self-absorption turnover is expected at a certain frequency ν_a (ν_* GHz) with the corresponding flux density S_* Jy.

Common to those BL Lac objects, a break or bending of the spectrum appears at the break frequency $\nu_b \approx 10^{15}$ Hz. The acceleration rate of relativistic electrons responsible for synchrotron radiation above ν_b may be smaller than the energy loss rate, making the energy spectrum steeper. Here the Lorentz factors of electrons which emit the synchrotron radiation at the turnover and break frequencies are denoted by γ_a and γ_b, respectively. Soft X-rays in the January epoch and the whole X-ray in the March epoch may be produced by the synchrotron radiation by electrons in the high-energy tail. The relatively flat, hard X-ray component seen in the January spectrum (see Fig. 2) may be attributed to the self-Compton photons. This self-Compton flux S_C has a power-law spectrum with the same spectral index as the synchrotron spectrum with

$$S_C \propto \nu_X^{-(p-1)/2}\theta_*^{-2(p+2)}\nu_*^{-(3p+7)/2}S_*^{(p+3)} \times [\delta/(1+z)]^{-(p+3)} \ln(\nu_b/\nu_a), \quad (1)$$

where ν_X is the frequency of a scattered photon, δ is the kinematical Doppler factor in the relativistic beaming model, z is the cosmological redshift, and the apparent angular diameter of the source is θ_* mas.

Energy densities of magnetic fields $u_{\rm mag}$ and synchrotron photons $u_{\rm syn}$, and the lower limit to the energy density of relativistic electrons $u_{\rm rel}^{\rm min}$, and γ_a are given as

$$u_{\rm mag} \propto \theta_*^8 \nu_*^{10} S_*^{-4}[\delta/(1+z)]^2, \quad (2)$$

$$u_{\rm syn} \propto \theta_*^{-2}\nu_* S_*[\delta/(1+z)]^{-4}, \quad (3)$$

$$u_{\rm rel}^{\rm min} \propto \theta_*^{-9}\nu_*^{-7}S_*^4[\delta/(1+z)]^{-5}(1+z)^2 d_{L^*}^{-1}, \quad (4)$$

and

$$\gamma_a \propto \theta_*^{-2}\nu_*^{-2}S_*[\delta/(1+z)]^{-1}, \quad (5)$$

respectively (Marscher *et al.* 1979; Marscher 1983). Here d_{L^*} G pc is the luminosity distance. The proportional coefficients in equations (1)–(5) are complicated functions of p. It is to be noted that resultant numerical values depend critically on the choices of θ_*, S_*, and ν_*, but the essential features described below are the same for plausible choices.

Since the X-ray flux by the self-Compton photons should be lower than the observed X-ray flux, we obtain the lower limit to the beaming factor $\delta_{\rm min}$ from equation (1) as

$$\delta_{\rm min} \propto (1+z)S_*\left[\frac{\ln(\nu_b/\nu_a)}{\nu_X^{(p-1)/2}\theta_*^{2(p+2)}\nu_*^{(3p+7)/2}S_*}\right]^{1/(p+3)}. \quad (6)$$

The synchrotron self-absorption turnover was not directly observed, but presumably ν_* lies at $\sim 10^3$, the intersection of straight extrapolation from radio and that from IR spectra. Assuming that the flux at the turnover is not much different from that of the smallest unresolved radio component (0.3 Jy with an angular size less than 0.3 mas), we adopt $S_* = 0.3$. The turnover frequency ν_* is determined so that the synchrotron flux gives the observed UV flux at 10^{15} Hz (6.5 mJy for the January epoch and 5.1 mJy for the March epoch), with the spectral index $\alpha = 0.625$ ($p = 2.25$) the well-fitted value to the IR-optical data. The source parameters are calculated as a function of θ_*, which are shown in Figure 5 for the January data. We notice that there are two critical values of θ_*, referred

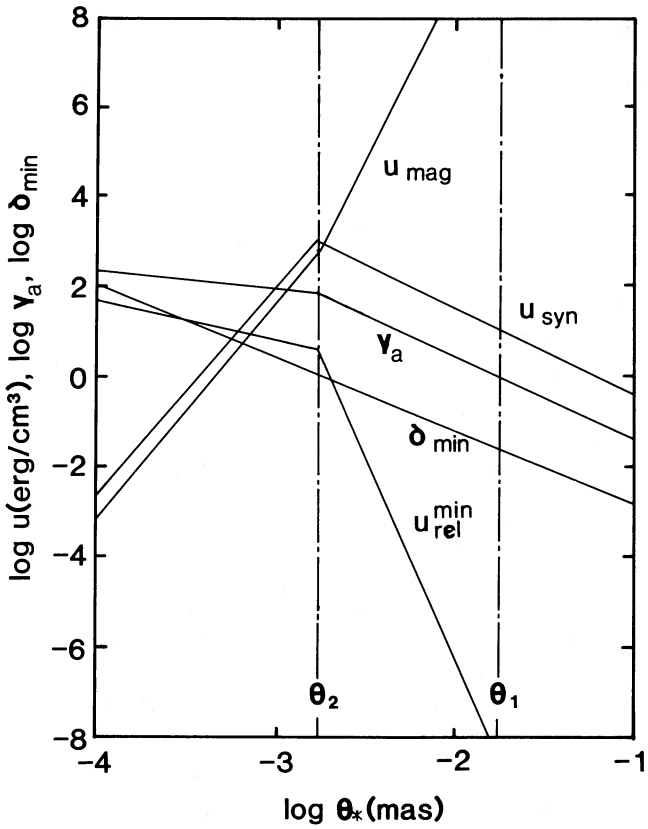

FIG. 5.—Source parameters obtained by the homogeneous synchrotron theory using the January data. The energy density of magnetic fields $u_{\rm mag}$, that of synchrotron photons $u_{\rm syn}$, and the lower limit to the energy density of relativistic electrons $u_{\rm rel}^{\rm min}$ are shown as a function of the angular diameter of the source θ_* mas. The minimum beaming factor $\delta_{\rm min}$ and the Lorentz factor of electrons γ_a which emit the synchrotron radiation at the self-absorption turnover frequency are also depicted.

TABLE 8

SOURCE CHARACTERISTICS DEDUCED FROM SYNCHROTRON SELF-COMPTON MODEL

PARAMETER	JANUARY OBSERVATION	MARCH OBSERVATIONS		
		1	2	3
ν_* (GHz)	2.2×10^3	1.5×10^3	1.5×10^3	1.5×10^3
θ_1 (mas)	1.6×10^{-2}	2.3×10^{-2}	2.3×10^{-2}	2.3×10^{-2}
θ_2 (mas)	1.8×10^{-3}	2.7×10^{-3}	2.7×10^{-3}	3.1×10^{-3}
δ	1	1	1.2	1.7
θ_* (mas)	1.8×10^{-3}	2.7×10^{-3}	2.4×10^{-3}	2.2×10^{-3}
t_{1c} (s)	7.6×10^4	1.2×10^5	1.0×10^5	9.7×10^4
γ_a	80	76	80	63
B (G)	1.3×10^2	9.5×10^1	7.0×10^1	7.9×10^1
$u_{\rm mag}$ (ergs cm^{-3})	6.4×10^2	3.6×10^3	2.0×10^2	2.5×10^2
$u_{\rm syn}$ (ergs cm^{-3})	1.2×10^3	4.0×10^2	2.1×10^2	5.7×10^1
$u_{\rm rel}$ (ergs cm^{-3})	3.1	1.2	1.4	3.9×10^{-1}
t_a (s)	3.3×10^2	1.1×10^3	1.8×10^3	8.5×10^3
t_b (s)	1.6×10^1	3.9×10^1	8.4×10^1	3.9×10^2

to as θ_1 and θ_2. For $\theta_* > \theta_1$, γ_a is less than unity. Since the synchrotron flux with a power-law spectrum is valid for $\gamma \gg 1$, thus θ_1 provides an optimistic upper limit to the angular diameter. While for $\theta_* < \theta_2$, the expected inverse Compton flux at ν_X deduced from the observed synchrotron flux exceeds the observed flux if $\delta = 1$. Conversely, such relativistic effects are required if θ_* is found virtually smaller than θ_2. In the second and third columns of Table 8, the results for the January and March data are tabulated for $\delta = 1$ and $\theta_* = \theta_2$, taking $\nu_X = 10^{18}$ Hz.

Ulrich *et al.* (1975) reported the absorption redshift of the underlying galaxy, $z = 0.03$, implying the distance of $90h^{-1}$ Mpc; 1 mas corresponds to $0.44h^{-1}$ pc, and the light crossing time of the source is $t_{1c} = 4.5 \times 10^7 \theta_* h^{-1}$ s, where h is the Hubble parameter in units of 100 km s^{-1} Mpc^{-1}. In Table 8 the cooling times, t_a and t_b, of electrons with Lorentz factors of γ_a and γ_b, are given, respectively, as well as t_{1c}. The cooling time of electrons responsible for the IR-optical radiation is shorter than the light crossing time, implying *in situ* acceleration of the relativistic electrons. The energy density of magnetic fields, $u_{\rm mag}$, dominates over that of relativistic electrons, if $u_{\rm rel}^{\rm min}$ is not so different from the true energy density of relativistic electrons, since γ_a is relatively small. This property is consistent with the observed behavior of polarization in the IR-optical bands that the position angle remained constant although the degree of polarization and flux varied with time.

Since VLBI experiments have shown ~ 1 mas structure at 5 GHz, radio structure should be more extended than IR-optical-UV component. This is consistent with the model of flat spectrum radio sources which can be expressed in terms of inhomogeneous synchrotron source (Marscher 1977; Konigl 1981). In this model the apparent angular size is inversely proportional to the frequency in the flat portion of the spectrum, and the size at 10^{12} Hz becomes $\sim 5 \times 10^{-3}$ mas, consistent with above analysis.

Mrk 421 was rather faint in the epochs of the present observation, and the total luminosity was $\sim 10^{44}$ ergs s^{-1}. At the most luminous epoch in the past it was ~ 10 times brighter. If we adopt the conclusion that the ultimate energy release occurs as a result of accretion onto the supermassive black hole and 10^{45} ergs s^{-1} corresponds to the Eddington luminosity, the mass of the black hole is $10^7\ M_\odot$ and the accretion energy is reprocessed in the size of 10^{13} cm, which amounts to $\theta_* \approx 10^{-5}$. Thus the size of the synchrotron source is $\sim 10^2$ times larger than the size of the ultimate energy release region.

b) *Spectral Variation*

Our January and March observations of Mrk 421 suggest that the self-Compton flux corresponding to the relatively flat, hard X-ray tail seen in the January observations decreased by more than factor of ~ 2 during 5 weeks, while the synchrotron flux decreased by 15%–25% in the IR, optical, and UV bands in the same interval. The radio flux remained essentially constant during those two observational periods. There seem to be several ways to explain the change of the spectra obtained in those two epochs with the homogeneous and spherical symmetric SSC model, as will be discussed below.

The simplest model is that the change was due to a slight steepening of the energy spectrum of electrons, while θ_*, S_*, and δ remained constant. Quantitatively, 22% decrease of synchrotron flux at 10^{15} Hz corresponds to the change of p from 2.25 to 2.33. This leads to decreases of $u_{\rm rel}^{\rm min}$ and $u_{\rm syn}$ by $\sim 10\%$ and $\sim 13\%$, respectively, while $u_{\rm mag}$ is increased by $\sim 3\%$ and ν_* remained essentially constant. The decrease of $S_{\rm C}$ depends on θ_* and is $\sim 20\%$ for $\theta_* \approx 3 \times 10^{-3}$, which is insufficient to explain the observed spectral change.

We also examined the cases where the spectral shape of electrons remained unchanged with $p = 2.25$. It is convenient to express S_* and ν_* in terms of θ_*, δ, $u_{\rm mag}$, and $u_{\rm rel}^{\rm min}$ from equations (2) and (4). Because the synchrotron flux $S_{\rm syn}$ is proportional to $S_* \nu_*^{(p-1)/2}$, then we obtain

$$S_{\rm syn} \propto (u_{\rm rel}^{\rm min})^{(p+4)/6} u_{\rm mag}^{(2p+5)/12} \theta_*^{(p+16/6} \delta^{(p+5)/2} . \quad (7)$$

On the other hand, the inverse Compton flux $S_{\rm C}$ is given from equation (1) as

$$S_{\rm C} \propto (u_{\rm rel}^{\rm min})^{(p+4)/3} u_{\rm mag}^{(p+7)/12} \theta_*^{(p+10)/3} \delta^{(p+5)/2} . \quad (8)$$

Let us first assume that δ and θ_* remained constant during the two epochs. The decreases of $S_{\rm syn}$ and $S_{\rm C}$ are due to those of $u_{\rm rel}^{\rm min}$ and $u_{\rm mag}$. A decrease of $u_{\rm mag}$, however, would lead to a larger decrease of $S_{\rm syn}$ than that of $S_{\rm C}$, contrary to the observed data. While a decrease of $u_{\rm rel}^{\rm min}$ would lead to a larger decrease of $S_{\rm C}$ than that of $S_{\rm syn}$. Quantitatively, $\sim 21\%$ decrease of $u_{\rm rel}^{\rm min}$ would decrease $S_{\rm syn}$ and $S_{\rm C}$ by $\sim 22\%$ and $\sim 40\%$, respectively. In this case S_* and ν_* would also decrease by $\sim 18\%$ and

$\sim 8\%$, respectively. The decrease of S_C is slightly smaller than the observed change.

We next consider the case of adiabatic expansion with $u_{mag} \propto \theta_*^{-4}$ and $u_{rel}^{min} \propto \theta_*^{-4}$. We obtain $S_{syn} \propto \theta_*^{-(7p+10)/6}$ and $S_C \propto \theta_*^{-(4p+13)/3}$. Then an expansion by $\sim 6\%$ would decrease S_{syn} and S_C by 22% and $\sim 35\%$, respectively. In this case S_* and ν_* would also decrease by $\sim 21\%$ and $\sim 13\%$, respectively. The decrease of S_C is also smaller than the observed change. A common feature to the above models is the decrease of the energy density of relativistic electrons.

Of course, there may exist more complicated changes involving the beaming factor δ. As an example, we assume that S_* remained constant because radio flux remained unchanged, which requires a 33% decrease of ν_* with constant $p = 2.25$. For $u_{mag} \propto \theta_*^{-4}$, we obtain $S_C \propto \nu_*^{(p-1)/6}\delta^{-(2p+7)/3}$. In order to decrease the self-Compton flux by a factor of 2.2, the kinematical Doppler factor is required to increase by 20% within 5 weeks, and the source would expand during the above time interval by 34%. Accompanying this u_{mag} and u_{rel}^{min} would decrease by a factor of 3.2 and 2.3, respectively. Thus the increase in the relativistic motion of the source might account for the observed property of the spectral variation separated by 5 weeks. This case is rather artificial since the increase of relativistic beaming compensates for a large decrease of intrinsic fluxes. In the third column of Table 8, the source parameters in the March epoch are shown assuming that the source in January was in a state of $\theta_* = \theta_2$ and $\delta = 1$. Since the hard X-ray spectrum was very steep in March, we obtain more severe constraint if we apply the same argument at higher ν_X. In the fourth column of Table 8 are tabulated the numerical results when we take $\nu_X = 1.4 \times 10^{18}$ Hz.

Virtually, the spectral variation in our two observational epochs may be explained by one or some combination of above alternative possibilities. It is also to be noted that the source should have some inhomogeneity. Even within the homogeneous source model discussed here, the radio emission arises in a more extended region than the central region where IR to UV emission emanates. In various inhomogeneous jet models, emissions at different frequencies are ascribed to different regions, implying different time scales of variations for different wave bands (Konigl 1981; Marscher 1980; Reynolds 1982; Ghisellini, Maraschi, and Treves 1985). However, our observations lack such detailed frequency dependence of time scales of flux variations, which does not enable us to set some constraints to inhomogeneous jet models. Only information we have obtained is the frequency independence of the degree of polarization at the March epoch, which is rather favorable to the homogeneous model. Although we have not applied the inhomogeneous jet models to determine source parameters and to explain the spectral variation, the analyses of our observations with such models are also awaited.

V. SUMMARY

The results of the present observations are summarized as follows:

1. Mrk 421 was in a relatively faint state in 1984 January and March at frequencies from IR through X-rays.

2. From January to March, Mrk 421 decreased its flux in the IR to X-ray bands. X-ray emission decreased by a factor of 2–3, while IR-UV radiation decreased by 15%–25%. Radio emission remained essentially stable.

3. The change in the X-ray spectral shape suggests that X-ray emission has two components: the soft component is probably the synchrotron radiation, and the hard component was more violently variable and may be ascribed to other mechanisms such as the inverse Compton scattering of synchrotron photons.

4. The break was observed at a frequency of $\sim 10^{15}$ Hz; the power-law index of IR-optical part is 0.5–0.8, while for the UV range it is ~ 1.0.

5. At the optical band, the degree of polarization showed a factor of 2 variation on the time scales of a few days, while the position angle remained constant during the present observations. The degree of polarization in the IR-optical region shows no wavelength dependence.

6. The radio spectrum is flat, and the extrapolation from the radio spectrum intersects the extrapolation from IR at a frequency of a few times 10^{12} Hz, below which the synchrotron self-absorption plays an important role.

7. Applying the homogeneous synchrotron source theory to the observed results, physical source parameters are deduced. Source size should be less than $\sim 10^{-2}$ mas. If the source size is less than a few times 10^{-3} mas, relativistic beaming is required. The source is magnetic field dominated, and the relativistic electrons with relatively low energy are responsible for the synchrotron radiation. The cooling time of electrons is shorter than the light crossing time, implying that there must be *in situ* acceleration of the electrons.

8. The spectral variations in the 5 week interval may be interpreted as a result of a slight steepening of the electron spectrum, the decrease of the energy density of relativistic electrons, an expansion of the source with or without an increase of beaming factor, or some combinations of these alternatives, although it is hard to discriminate those possibilities.

Some of the optical observations at Okayama were kindly made for this program by K. Misawa, Y. Fujime, and M. Kondo. The IR data at January 30 and February 4 and 6 were kindly provided by E. I. Robson. We appreciate their cooperation. The work at the University of Michigan was supported by the National Science Foundation under grant AST 83-01234. The authors would like to appreciate the referee for suggestions regarding emission models.

REFERENCES

Aaronson, M. 1978, *Ap. J.* (*Letters*), **221**, L103.
Allen, D. A. 1976, *Ap. J.*, **207**, 367.
Baath, L. B. 1984, in *IAU Symposium 110, VLBI and Compact Radio Sources*, ed. R. Fanti, K. Kellerman, and G. Setti (Dordrecht: Reidel), p. 127.
Baath, L. B., Elgered, G., Lundqvist, G., Graham, D., Weiler, K. W., Seielstad, G. A., Tallqvist, S., and Schilizzi, R. T. 1981, *Astr. Ap.*, **96**, 316.
Bailey, J., Cunningham, E. C., Hough, J. H., and Axon, D. J. 1981, *M.N.R.A.S.*, **197**, 627.
Blackwell, D. E., Leggett, S. K., Petford, A. D., Mountain, C. M., and Selby, M. J. 1983, *M.N.R.A.S.*, **205**, 897.
Blandford, R. D. 1984, in *11th Texas Symposium on Relativistic Astroophysics*, ed. D. S. Evans (*Ann. NY Acad. Sci.*), **422**, 303.
Bregman, J. N., *et al.* 1982, *Ap. J.*, **253**, 19.
———. 1984, *Ap. J.*, **276**, 454.
Frogel, J. A., Persson, S. E., Aaronson, M., Becklin, E. E., Matthews, K., and Neugebauer, G. 1975, *Ap. J.* (*Letters*), **200**, L123.
Frogel, J. A., Persson, S. E., Aaronson, M., and Matthews, K. 1978, *Ap. J.*, **220**, 75.
Ghisellini, G., Maraschi, L., and Treves, A. 1985, *Astr. Ap.*, **146**, 204.
Glass, I. S. 1984, *M.N.R.A.S.*, **211**, 461.
Glassgold, A. E., *et al.* 1983, *Ap. J.*, **274**, 101.
Gould, R. J. 1979, *Astr. Ap.*, **76**, 306.
Hagen-Thorn, V. A., Marchenko, S. G., Smehacheva, R. I., and Yakovleva, V. A. 1983, *Astrophyzika*, **19**, 199.

Hearn, D. R., Marshall, F. J., and Jernigen, J. R. 1979, *Ap. J.* (*Letters*), **227**, L63.
Hickson, P., Fahlman, G. G., Auman, J. R., Walker, G. A. H., Menon, T. K., and Ninkov, Z. 1982, *Ap. J.*, **258**, 53.
Hutter, D. J., and Mufson, S. L. 1986, *Ap. J.*, **301**, 50.
Impey, C. D. 1983, *M.N.R.A.S.*, **202**, 397.
Johnson, H. L. 1966, *Ap. J.*, **143**, 87.
Joyce, R. R., and Simon, M. 1976, *Pub. A.S.P.*, **88**, 870.
Kapahi, V. K. 1979, *Astr. Ap.*, **74**, L11.
Kikuchi, S., and Mikami, Y. 1986, *Pub. Astr. Soc. Japan*, in press.
Kinman, T. D. 1978, in *Pittsburgh Conference on BL Lac Objects*, ed. A. M. Wolfe (Pittsburgh: University of Pittsburgh), p. 82.
Kondo, Y., *et al.* 1981, *Ap. J.*, **243**, 690.
Konigl, A. 1981, *Ap. J.*, **243**, 700.
Koyama, K., *et al.* 1984, *Pub. Astr. Soc. Japan.*, **36**, 659.
Marscher, A. P. 1977, *Ap. J.*, **216**, 244.
———. 1980, *Ap. J.*, **235**, 386.
———. 1983, *Ap. J.*, **264**, 296.
Marscher, A. P., Marshall, F. E., Mushotzky, R. F., Dent, W. A., Balonik, T. J., and Hartman, M. F. 1979, *Ap. J.*, **233**, 498.
Margon, B., Jones, T. W., and Wardle, J. F. C. 1978, *A.J.*, **83**, 1021.
Maza, J., Martin, P. G., and Angel, J. R. P. 1978, *Ap. J.*, **224**, 368.
Mufson, S. L., *et al.* 1980, *Ap. J.*, **241**, 74.
———. 1984, *Ap. J.*, **285**, 571.
Mushotzky, R. F., Boldt, E. A., Holt, S. S., and Serlemitsos, P. J. 1979, *Ap. J.* (*Letters*), **232**, L17.
O'Dell, S. L., Puschell, J. J., Stein, W. A., Owen, F., Porcas, R. W., Mufson, S., Moffet, T. J., and Ulrich, M. H. 1978*a*, *Ap. J.*, **224**, 22.
O'Dell, S. L., Puschell, J. J., Stein, W. A., and Warner, J. W. 1978*b*, *Ap. J. Suppl.*, **38**, 267.
Persson, S. E., Frogel, J. A., and Aaronson, M. 1979, *Ap. J. Suppl.*, **39**, 61.
Reynolds, S. P. 1982, *Ap. J.*, **256**, 13.
Riegler, G. R., Agrawal, P. C., and Mushotzky, R. F. 1979, *Ap. J.* (*Letters*), **233**, L47.
Tanaka, Y., *et al.* 1984, *Pub. Astr. Soc. Japan*, **36**, 641.
Ulrich, M. H., Hackney, K. R. H., Hackney, R. H., and Kondo, Y. 1984, *Ap. J.*, **276**, 466.
Ulrich, M. H., Kinman, T. D., Lynds, C. R., Rieke, G. H., and Eckers, R. D. 1975, *Ap. J.*, **198**, 261.
Ulvestad, J. S., Johnston, K. J., and Weiler, K. W. 1983, *Ap. J.*, **266**, 18.
Urry, C. M., Mushotzky, R. F., and Holt, S. S. 1986, *Ap. J.*, **305**, 369.
Warwick, R. S., McHardy, I. M., and Pounds, K. A. 1985, *Space Sci. Rev.*, **40**, 597.
Wehrle, A. E., Preston, R. A., Meier, D. L., Gorenstein, M. V., Shapiro, I. I., Rogers, A. E. E., and Rius, A. 1984, *Ap. J.*, **284**, 18.
Weiler, K. W., and Johnston, K. J. 1980, *M.N.R.A.S.*, **190**, 269.
Wills, B. J., *et al.* 1983, *Ap. J.*, **274**, 62.
Worrall, D. M., Boldt, E. A., Holt, S. S. Mushotzky, R. F., and Serlemitsos, P. J. 1981, *Ap. J.*, **243**, 53.
Worrall, D. M., *et al.* 1982, *Ap. J.*, **261**, 403.
———. 1984*a*, *Ap. J.*, **278**, 521.
———. 1984*b*, *Ap. J.*, **284**, 512.
Worrall, D. M., Puschell, J. J., Rodrigues-Espinosa, J. M., Bruhweiler, F. C., Miller, H. R., Aller, M. F., and Aller, H. D. 1984*c*, *Ap. J.*, **286**, 711.

H. D. ALLER and M. F. ALLER: Department of Astronomy, Dennison Building, University of Michigan, Ann Arbor, MI 48109-1090

P. BRAND and J. BURNELL: Astronomy Department, University of Edinburgh, Blackford Hill, Edinburgh, EH9 3HJ, Scotland, UK

K. R. HACKNEY and R. L. HACKNEY: Department of Physics and Astronomy, Western Kentucky University, TCCW119, Bowling Green, KY 42101

S. HAYAKAWA: Department of Astrophysics, Nagoya University, Furo-cho Chikusa-ku, Nagoya 464, Japan

N. HIROMOTO: Radio Research Laboratory, 2-1, Nukuikitamachi 4-chome, Koganei, Tokyo 184, Japan

R. HOSHI: Department of Physics, Rikkyo University, 34-1, Nishi-Ikebukuro 3-chome, Toshima-ku, Tokyo 171, Japan

H. INOUE, K. KOYAMA, F. MAKINO, K. MAKISHIMA, M. MATSUOKA, and Y. TANAKA: Institute of Space and Astronautical Science, 6-1, Komaba 4-chome, Meguro-ku, Tokyo 153, Japan

M. INOUE and F. TAKAHARA: Nobeyama Radio Observatory, Tokyo Astronomical Observatory, University of Tokyo, Nobeyama, Minamisaku, Nagano 384-13, Japan

T. KATO and H. TABARA: Faculty of Education, Utsunomiya University, 350, Minemachi, Utsunomiya, Tochigi 321, Japan

S. KIKUCHI and Y. MIKAMI: Tokyo Astronomical Observatory, University of Tokyo, 21-1, Osawa 2-chome, Mitaka, Tokyo 181, Japan

Y. KONDO: Laboratory for Astronomy and Solar Physics, NASA/Goddard Space Flight Center, Code 685, Greenbelt, MD 20771

S. L. MUFSON: Department of Astronomy, Indiana University, 319 Swain West, Bloomington, IN 47405

M. NISHIDA: Department of Physics, Kyoto University, Kitashirakawa-Oiwakecho, Sakyo-ku, Kyoto 606, Japan

M. G. SMITH and P. M. WILLIAMS: Royal Observatory Edinburgh, Blackford Hill, Edinburgh, EH9 3HJ, Scotland, UK

M. TSUBOI: Department of Astronomy, University of Tokyo, 11-16, Yayoi, 2-chome, Bunkyo-ku, Tokyo 113, Japan

C. M. URRY: Center for Space Research, Massachusetts Institute of Technology, Cambridge, MA 02139

W. Z. WISNIEWSKI: Lunar and Planetary Laboratory, University of Arizona, Tucson, AZ 85721